

Nogo-B Receptor Modulates Angiogenesis Response of Pulmonary Artery Endothelial Cells Through eNOS Coupling

Ru-Jeng Teng^{1,4,5}, Ujala Rana^{2,3,4}, Adeleye J. Afolayan^{1,4,5}, Baofeng Zhao^{2,3,4}, Qing R. Miao^{2,3,4}, and Girija G. Konduri^{1,4,5}

Departments of ¹Pediatrics, ²Surgery, ³Pathology, ⁴Children's Research Institute, and ⁵Cardiovascular Research Center, Medical College of Wisconsin, Milwaukee, Wisconsin

Abstract

Nogo-B, a reticulon-4 isoform, modulates the motility and adhesion of vascular endothelial cells after binding to its receptor, Nogo-B receptor (NgBR). Nogo-B/NgBR pathway contributes to vascular remodeling and angiogenesis, but the role of this pathway in the angiogenesis of developing lungs remains unknown. We previously reported that angiogenesis function of pulmonary artery endothelial cells (PAECs) is impaired by increased reactive oxygen species formation in a fetal lamb model of intrauterine pulmonary hypertension (IPH). Here, we report that Nogo-B/NgBR pathway is altered in IPH, and that decreased NgBR expression contributes to impaired angiogenesis in IPH. We observed a decrease in NgBR levels in lysates of whole lung or PAECs from fetal lambs with IPH compared with controls. Overexpression of NgBR in IPH PAECs rescued the *in vitro* angiogenesis defects and increased the phosphorylation of both Akt and endothelial nitric oxide synthase at serine¹¹⁷⁹ as well as the levels of both manganese superoxide dismutase and GTP cyclohydrolase-1. Consistent with the phenotype of IPH PAECs, knockdown of NgBR in control PAECs decreased the

levels of nitric oxide, increased the levels of reactive oxygen species, and impaired *in vitro* angiogenesis. Our data demonstrate that NgBR mediates PAEC angiogenesis response through the modulation of Akt/endothelial nitric oxide synthase functions, and its decreased expression is mechanistically linked to IPH-related angiogenesis defects in the developing lungs.

Keywords: Nogo-B; Nogo-B receptor; intrauterine pulmonary hypertension; pulmonary artery endothelial cells; angiogenesis

Clinical Relevance

We report a previously unexplored role of Nogo-B receptor (NgBR) in endothelial nitric oxide synthase coupling and angiogenesis of developing lungs. Our finding not only expands our knowledge of NgBR in lung development, but also provides a new therapeutic target for future research that may help our management in infants suffering from persistent pulmonary hypertension of the newborn.

Reticulons (RTNs) are a family of proteins that share a common C-terminal domain, and are particularly abundant in the endoplasmic reticulum (1, 2). RTN-4, also known as neurite outgrowth inhibitor (Nogo), is an RTN protein encoded by RTN-4 gene in humans (3, 4). Three different isoforms (Nogo-A, -B, and -C) have been identified as the end products resulting from differential splicing, differential promoter

usage, and encoding (5, 6). Some isoforms, like Nogo-B, have more than one subisoform, such as Nogo-B1 and Nogo-B2 (1, 7). Nogo-A and Nogo-C are highly expressed in the central nervous system, with Nogo-C being additionally found in the skeletal muscle. Nogo-A, and probably also Nogo-C (8), appear to be neuron-specific inhibitors of axonal regeneration. In contrast, Nogo-B is widely distributed in the nervous system,

vessel wall, heart, spleen, skeletal muscle, and testis (1, 9). Nogo-B acts as a chemoattractant for endothelial cells, similar to vascular endothelial growth factor (VEGF), and antagonizes the platelet-derived growth factor-stimulated migration of smooth muscle cells (10). Marked neointimal expansion and defects in ischemia-induced arteriogenesis and angiogenesis occur in Nogo-A/B-deficient mice, suggesting that

(Received in original form June 30, 2013; accepted in final form February 9, 2014)

This work was supported by National Institutes of Health grant RO3HD073274 and Clinical and Translational Science Institute pilot grant (R.-J.T.), American Heart Association postdoctoral fellowship (B.Z.), RO1HL108938 (Q.R.M.), RO1HL057268 (G.G.K.), and RO3 HD065841 (G.G.K.), and Muma Endowed Chair in Neonatology (G.G.K.).

Correspondence and requests for reprints should be addressed to Ru-Jeng Teng, M.D., Division of Neonatology, Department of Pediatrics, Medical College of Wisconsin, Suite C410, Children Corporate Center, 999N 92nd Street, Wauwatosa, WI 53226. E-mail: rteng@mcw.edu

This article has an online supplement, which is accessible from this issue's table of contents at www.atsjournals.org

Am J Respir Cell Mol Biol Vol 51, Iss 2, pp 169–177, Aug 2014

Copyright © 2014 by the American Thoracic Society

Originally Published in Press as DOI: 10.1165/rcmb.2013-0298OC on February 25, 2014

Internet address: www.atsjournals.org

Nogo-B has a protective role in blood vessel homeostasis (11). Nogo-B receptor (NgBR) was identified as a specific receptor essential for Nogo-B-stimulated chemotaxis and morphogenesis of endothelial cells (10, 12). Morpholino-mediated NgBR knockdown in zebrafish blocks intersomitic vessel formation, indicating a critical role for Nogo-B/NgBR signaling pathway in blood vessel development (13).

Persistent pulmonary hypertension of the newborn (PPHN) is a disease of neonates, characterized by decreased blood vessel density and/or impaired pulmonary vasodilation (14). Prenatal constriction of ductus arteriosus in the fetal lamb creates persistent intrauterine pulmonary hypertension (IPH), and is the most commonly used animal model to study PPHN (15). We previously reported that pulmonary artery endothelial cells (PAECs) isolated from IPH lungs show increased reactive oxygen species (ROS) formation and endothelial nitric oxide (NO) synthase (eNOS) uncoupling (16, 17) as compared with control PAECs. IPH PAECs also show impaired *in vitro* and *ex vivo* angiogenesis, which may contribute to the histological and physiological changes in PPHN (18). We also reported that expression and activity of manganese superoxide dismutase (MnSOD) are decreased in IPH PAECs, which further increased ROS formation (19). Nogo-A is known to antagonize ROS generation and protects premature cortical neurons (20). The role of Nogo-B/NgBR in ROS generation and pulmonary blood vessel formation remains unknown. A recent study reported that hypoxia induces Nogo-B expression in smooth muscle cells of the mouse pulmonary arteries, and serum levels of Nogo-B were also found to be increased in patients with idiopathic pulmonary hypertension (21). However, alterations in Nogo-B/NgBR signaling and its mechanistic link to oxidative stress in PPHN remain unexplored.

In the current study, we investigated the role of NgBR in regulating angiogenesis response of PAECs from developing lungs and alterations in NgBR signaling in IPH, using PAECs from fetal lambs with or without IPH. We observed that (1) NgBR is involved in modulating fetal PAEC angiogenesis; (2) activation of eNOS is involved in NgBR-modulated angiogenesis; and (3) IPH is associated with altered NgBR expression, angiogenesis, and eNOS activity in PAECs. Our results demonstrate that NgBR is

important for the *in vitro* angiogenesis of PAECs from developing lungs.

Materials and Methods

Animal studies were approved by the Medical College of Wisconsin

Institutional Animal Care and Use Committee. Identity of PAECs was verified by factor VIII antigen (22) and acetylated low density lipoprotein uptake (23). Right upper lobe lung tissue was obtained for Western blotting and for immunofluorescence staining.

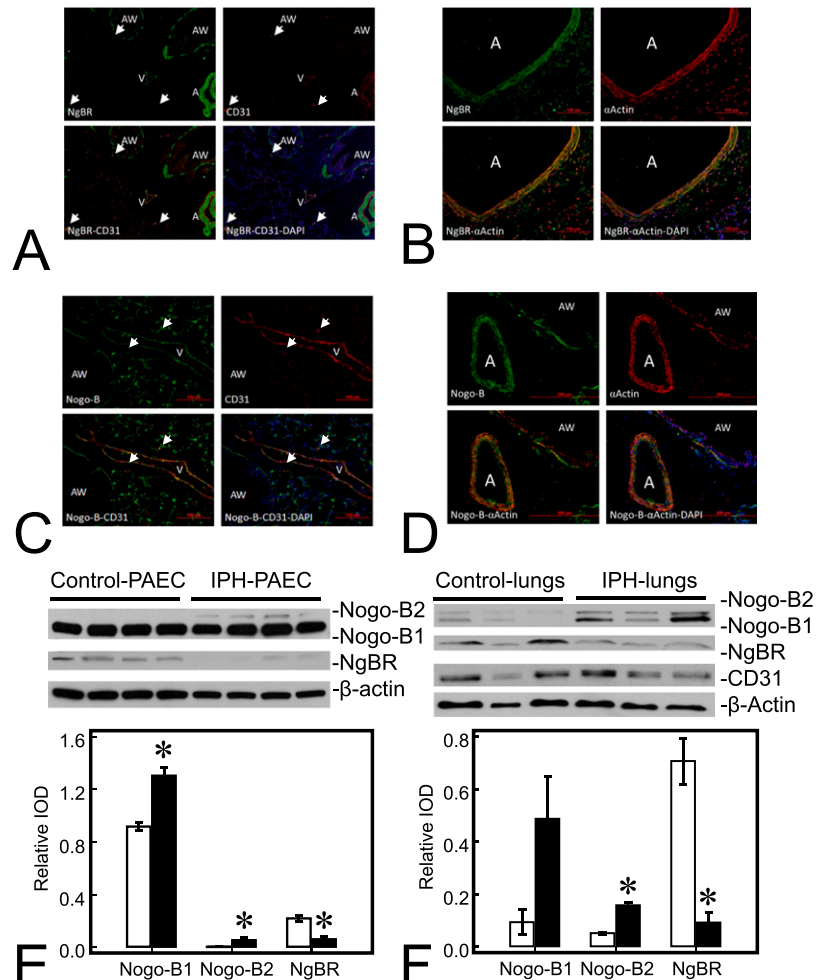


Figure 1. Nogo-B receptor (NgBR) and its ligand, Nogo-B (NgB), are widely distributed in fetal sheep lungs. (A) NgBR (green) is detected in airway (AW), artery (A), and vein (V) in lung sections; CD31 (red) staining is in the endothelial lining of pulmonary vessels (A and V); colocalization of NgBR and CD31 (yellow) is observed in the lining of A and V, indicating endothelial localization of NgBR. (B) NgBR (green) and smooth muscle α -actin (red) colocalize (yellow) in the muscular layer of A, indicating smooth muscle location of NgBR. (C) Nogo-B (green) is also widely distributed in the lung, including A, V, pneumocytes, and AW, and colocalizes (yellow) with CD31 (red) of a vein in this section. (D) Nogo-B is also distributed in smooth muscle cells (red) of A and AW. Nogo-B level is increased, whereas NgBR level is decreased in pulmonary artery endothelial cells (PAECs) and lungs from lambs with intrauterine pulmonary hypertension (IPH). (E) Levels of both Nogo-B1 and Nogo-B2, subisoforms of Nogo-B, are increased in IPH PAECs (1.42-fold and 14.8-fold for Nogo-B1 and Nogo-B2, respectively) compared with control PAECs. The level of NgBR decreased by roughly 72% in IPH-PAECs compared with control PAECs. (F) Similar to PAECs, levels of Nogo-B1 and Nogo-B2 were also increased in IPH lungs (5.44-fold and 2.98-fold for Nogo-B1 and Nogo-B2, respectively), whereas the level of NgBR was decreased by roughly 87%. The findings are similar when using CD31 as the loading control. Data are shown as mean (\pm SE). Open bar, control; closed bar, IPH; white arrow, microvasculature. $*P < 0.05$ compared with control PAECs or lungs. IOD, integrated optical density.

Antibodies and Chemicals

NgBR rabbit monoclonal antibody was from Epitomics (Burlingame, CA). Nogo-B rabbit antibody was from Imgenex (San Diego, CA). Recombinant human VEGF was obtained from National Cancer Institute at Frederick–Biological Resources Branch of the National Cancer Institute (Frederick, MD).

NgBR Overexpression Plasmid DNA

Human NgBR cDNA was cloned into pIRES-neo vector (Clontech, Mountain View, CA) as described previously (12).

Design of NgBR Small Interfering RNA and Primers for RT-PCR

NgBR small interfering RNA (siRNA) and primers were designed according to the conserved regions of mRNAs (12) and are detailed in the online supplement.

NgBR Overexpression and Knockdown

NgBR overexpression and knockdown were performed according to manufacturer's protocol and are detailed in the online supplement.

Akt Activation

Akt is activated by phosphorylation at Thr³⁰⁸. Phospho-Akt then activates eNOS by phosphorylation at Ser¹¹⁷⁹ (24). PAECs were serum starved and then stimulated with VEGF (10 ng/ml). Akt and phospho-Akt levels were quantified by Western blotting.

Western Blotting

PAECs and lung lysates were homogenized in 3-(N-Morpholino)propanesulfonic acid, 4-Morpholinepropanesulfonic acid (MOPS) buffer and lysate protein was resolved by SDS-PAGE as detailed in the online supplement. Low temperature electrophoresis was used to study eNOS dimer formation (25). Phosphorylation of eNOS was normalized to the corresponding total eNOS protein levels.

Immunohistochemistry Staining

Fetal sheep lung was inflated with 10% formalin for fixation. Paraffin sections were deparaffinized, and blocked with serum (Dako, Carpinteria, CA) for 30 minutes before staining with primary antibodies. Alexa-Fluor–conjugated antibody was applied as the secondary antibody.

In vitro Angiogenesis Assays

The *in vitro* angiogenesis assays were performed as we previously reported

(18, 25) and detailed in the online supplement.

Measurements of NO and ROS Levels

NO and ROS levels were quantified using 4-amino-5-methylamino-2', 7'-difluorofluorescein diacetate (DAF-FM-DA) and dihydroethidium (DHE), respectively, as we previously described (18, 26, 27) and detailed in the online supplement. Data for stimulated NO₂⁻ + NO₃⁻ levels were normalized to the corresponding protein levels (25).

MnSOD Activity Assay

MnSOD-specific activity was measured using a colorimetric assay (Cayman Chemical, Ann Arbor, MI) and was normalized to the protein content (19). Absorbance was read at 450 nm.

Statistical Analysis

Data are shown as mean (\pm SE). Student's *t* test, or Mann-Whitney U test, was used for comparing two groups wherever appropriate. ANOVA with Newman-Keuls *post hoc* test was used to compare data from more than two groups. A *P* value of less than 0.05 was considered statistically significant.

Results

Distribution of Nogo-B and NgBR in the Lung

NgBR and its ligand, Nogo-B, are both widely distributed in fetal sheep lungs (Figures 1A–1D), including endothelial cells of the arteries and veins, epithelial cells of the airway, and pneumocytes in alveoli. Colocalization of NgBR (*green*) and CD31 (*red*) indicates endothelial distribution of NgBR (Figure 1A). Colocalization of NgBR (*green*) and smooth muscle α -actin (*red*) indicates smooth muscle distribution of NgBR (Figure 1B). Similar colocalization with CD31 and α -actin was also observed for Nogo-B (Figures 1C and 1D, *green*).

Nogo-B/NgBR Expression Is Altered in IPH

Two bands were observed in Western blot for Nogo-B, the ligand for NgBR, in lysates from both PAECs and lung homogenates (Figures 1E and 1F), similar to previous reports in the literature (7). The expression of Nogo-B was higher in IPH PAECs than in controls (1.32 ± 0.15 versus 0.92 ± 0.09 for Nogo-B1; 0.11 ± 0.03 versus

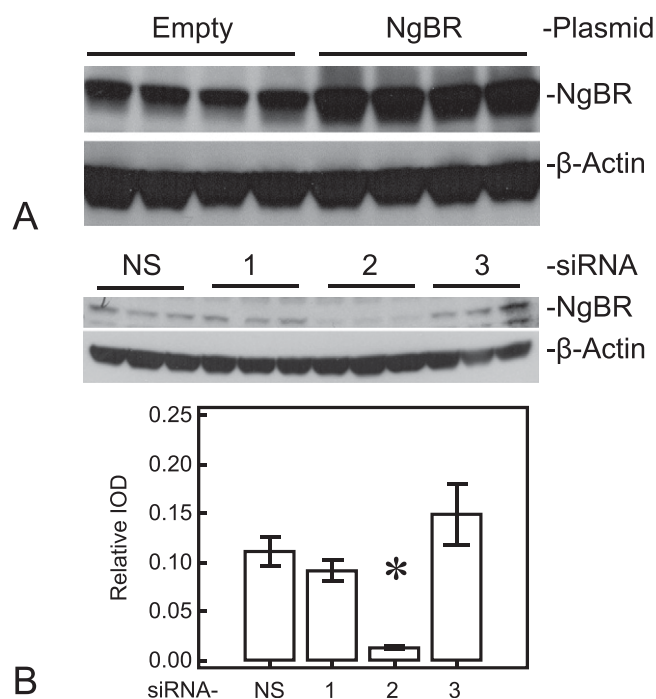


Figure 2. NgBR plasmid effectively increases NgBR level in IPH PAECs and small interfering RNA (siRNA) for NgBR decreases NgBR level in control PAECs. (A) Plasmid containing hemagglutinin-tagged human NgBR increased NgBR level by almost 40%. (B) Among the three siRNAs designed against NgBR, siRNA-2 decreased the NgBR level (\sim 10-fold) in control PAECs. NS, nonsilencing siRNA; 1–3 refer to corresponding siRNAs. **P* < 0.05 compared with NS siRNA. Data are shown as mean (\pm SE).

0.01 ± 0.01 for Nogo-B2; $n = 4$, $P < 0.05$), whereas the expression of its receptor, NgBR, was lower in IPH PAECs than controls (0.06 ± 0.01 versus 0.29 ± 0.01 ; $n = 4$, $P < 0.05$, Figure 1E). Similar to *in vitro* results, Nogo-B expression in IPH lungs was also higher than controls (0.49 ± 0.16 versus 0.09 ± 0.05 for Nogo-B1, $P = 0.08$; 0.158 ± 0.010 versus 0.053 ± 0.004 for Nogo-B2, $n = 3$, $P < 0.05$), whereas, NgBR expression in IPH lungs was lower than controls (0.09 ± 0.04 versus 0.71 ± 0.09 ; $n = 3$, $P < 0.05$; Figure 1F). The results were identical using either β -actin or CD31 as the loading control.

NgBR Expression Modulates *In Vitro* Angiogenesis of PAECs

To explore the role of NgBR in the impaired angiogenesis previously observed in IPH, we overexpressed NgBR in IPH PAECs or knocked down NgBR in control PAECs. NgBR overexpression in IPH PAECs increased the NgBR expression by roughly 40% (0.75 ± 0.25 versus 0.53 ± 0.05 ; $n = 4$, $P < 0.05$), but did not affect Nogo-B

expression (Figure 2A). We attempted NgBR knockdown using three different siRNAs in control PAECs, as described in MATERIALS AND METHODS, and found that only one of them, siRNA-2, significantly decreased endogenous NgBR expression by roughly 10-fold (0.013 ± 0.002 versus 0.111 ± 0.015 ; $n = 3$, $P < 0.05$; Figure 2B) and mRNA levels by roughly 90%. Consistent with the expression pattern of NgBR and Nogo-B in IPH PAECs, knockdown of NgBR in control PAECs also increased Nogo-B1 expression (0.27 ± 0.01 versus 0.51 ± 0.01 ; $n = 3$, $P < 0.05$; Figure 2B). We used siRNA-2 subsequently for the angiogenesis, NO, and ROS studies in control cells.

NgBR overexpression in IPH PAECs increased tube formation to $240.5 (\pm 13.8)\%$ when compared with IPH PAECs alone ($n = 10$, $P < 0.05$; Figure 3A). The gaps for scratch recovery decreased from $760.5 (\pm 29.3) \mu\text{m}$ to $572.9 (\pm 13.4) \mu\text{m}$ ($n = 12$, $P < 0.05$; Figure 3B) with NgBR overexpression. These observations suggest that restoring NgBR expression can rescue

the impaired angiogenesis and migration responses of IPH PAECs.

NgBR knockdown in control PAECs decreased the tube formation to $41.5 (\pm 2.9)\%$ of nonsilencing (NS) siRNA transfected controls ($n = 6$, $P < 0.05$; Figure 3C). The gaps for scratch recovery increased from $363.2 (\pm 10.1)$ to $538.4 (\pm 15.6) \mu\text{m}$ ($n = 12$, $P < 0.05$; Figure 3D) with NgBR knockdown in control PAECs, suggesting that knockdown of NgBR can recapitulate the angiogenesis defects observed in IPH PAECs. NgBR knockdown did not affect cell viability and growth by 6 and 24 hours (Figure 3E). These results suggest that NgBR is essential for maintaining the migration and angiogenesis functions of PAECs.

NgBR Expression Modulates NO and ROS Formation in PAECs

We previously reported that IPH PAECs have decreased NO and increased ROS levels due to eNOS uncoupling (26) and increased reduced nicotinamide adenine dinucleotide phosphate (NADPH) oxidase

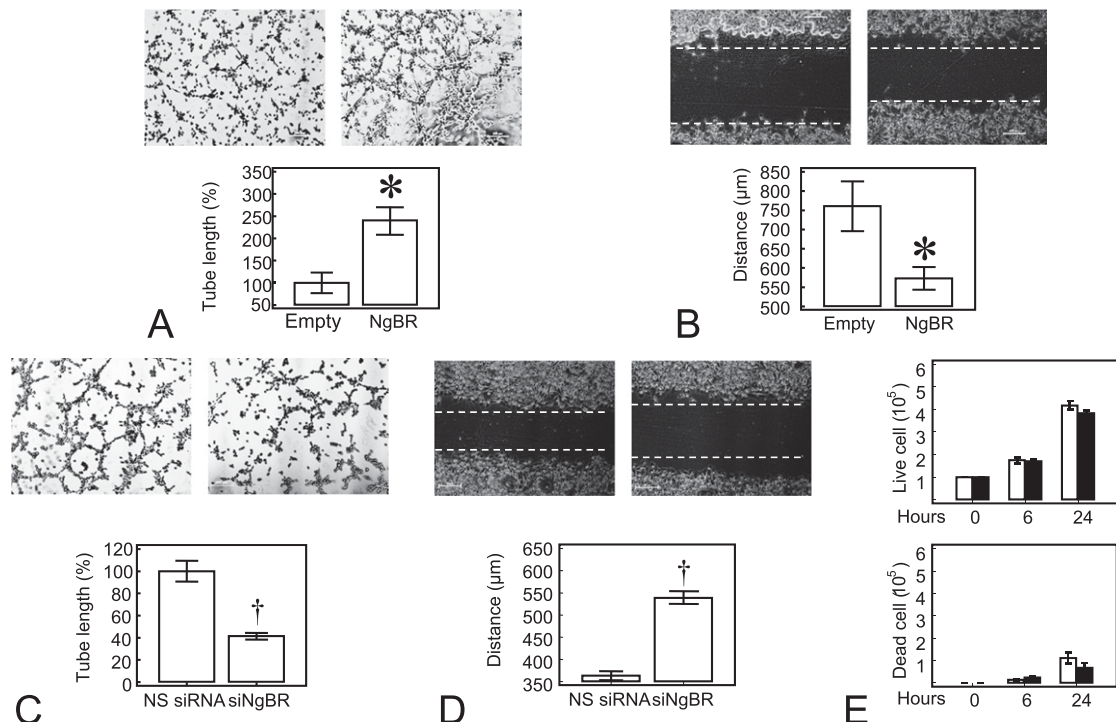


Figure 3. Altered NgBR level affects *in vitro* angiogenesis in PAECs. (A) Baseline *in vitro* tube formation was impaired in IPH PAECs; NgBR overexpression rescued the *in vitro* tube formation defects of IPH PAECs. (B) NgBR overexpression increased the migration of IPH PAECs, as demonstrated by the decreased gap for IPH PAECs overexpressing NgBR. (C) NgBR knockdown with siRNA-2 impaired *in vitro* tube formation of control PAECs. (D) NgBR knockdown decreased the migration of control PAECs, as demonstrated by increased gap for control PAECs treated with NgBR siRNA-2. (E) NgBR knockdown did not affect cell viability and growth. Open bar, control; closed bar, NgBR knockdown. * $P < 0.05$ compared with empty plasmid; † $P < 0.05$ compared with NS siRNA. Data are shown as mean (\pm SE).

activity (25). We examined whether the decreased NgBR expression in IPH PAECs is related to altered NO and ROS formation using DAF and DHE staining, respectively, as described previously (25, 26). As shown in Figure 4A, NgBR overexpression in IPH PAECs increased the DAF fluorescence from $2.84 (\pm 0.30) \times 10^6$ relative light unit (RLU) to $10.82 (\pm 1.36) \times 10^6$ RLU ($n = 5, P < 0.05$, Figure 4A) whereas DHE fluorescence decreased from $5.72 (\pm 0.62) \times 10^6$ RLU to $4.13 (\pm 0.61) \times 10^6$ RLU

($n = 8, P < 0.05$; Figure 4B). Consistent with the epifluorescence results, NgBR overexpression increased the total $\text{NO}_2^- + \text{NO}_3^-$ levels and decreased the levels of 2-hydroxy-ethidium, a specific marker for O_2^- . Total $\text{NO}_2^- + \text{NO}_3^-$ levels in IPH PAECs with NgBR overexpression, empty plasmid, and NgBR overexpression with L-N^G-nitroarginine (L-NNA) treatment were $29.6 (\pm 4.7)$ pmoles/mg total protein, $13.4 (\pm 1.2)$ pmoles/mg total protein, and $11.0 (\pm 1.5)$ pmoles/mg total

protein, respectively ($n = 6, P < 0.05$ by AONVA). 2-Hydroxy-ethidium levels, reflecting O_2^- formation, decreased in IPH PAECs after NgBR overexpression (0.021 ± 0.003 nmoles/mg protein) as compared with empty plasmid control (0.030 ± 0.002 nmoles/mg protein) ($n = 6, P < 0.05$). No statistical difference in other indicators ($\text{E}^+ - \text{E}^+$, HE- E^+ , HE-HE, and E^+) of ROS was observed ($P > 0.5$).

NgBR knockdown in control PAECs decreased DAF fluorescence from

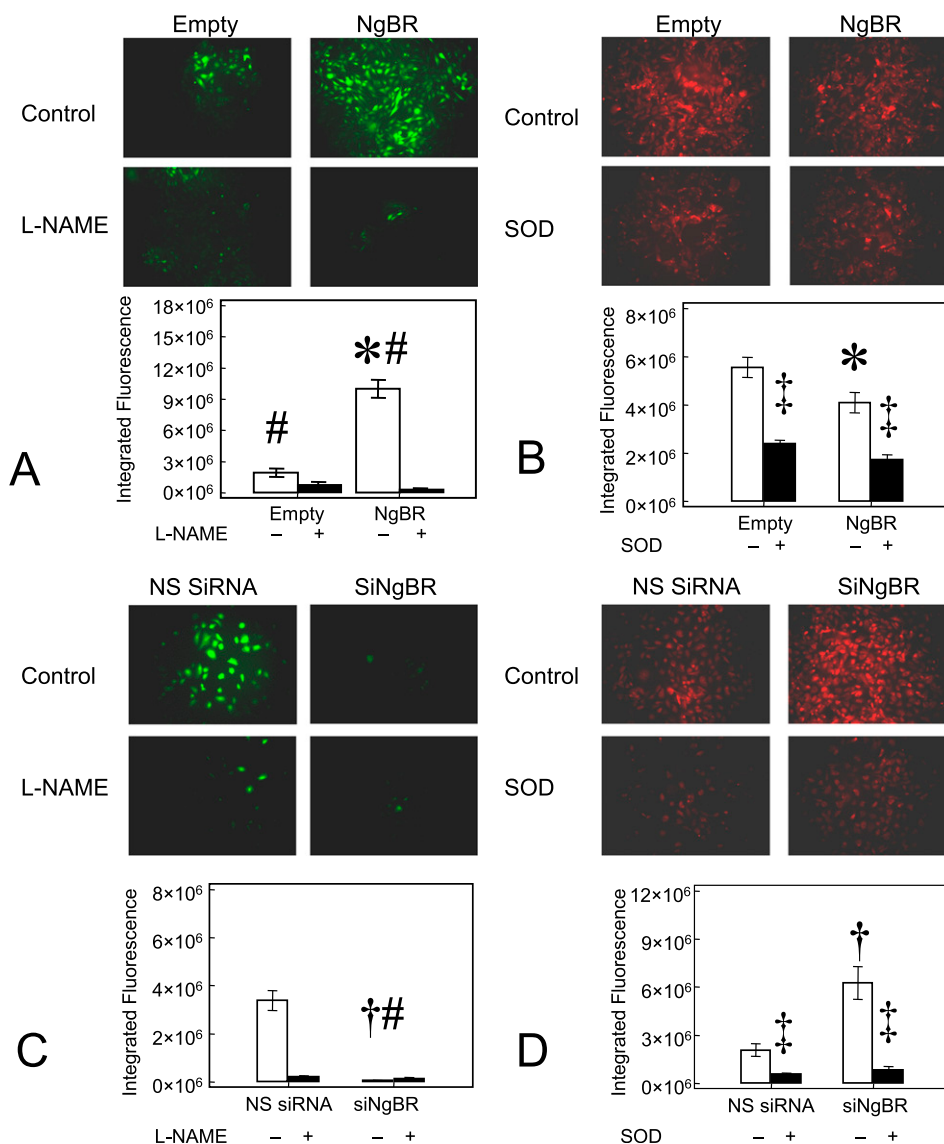


Figure 4. Altered NgBR level affects nitric oxide (NO) and reactive oxygen species (ROS) formation in PAECs. (A) NgBR overexpression in IPH PAECs increased 4-amino-5-methylamino-2', 7'-difluorofluoresceine (DAF) fluorescence, indicating increased NO formation. (B) NgBR overexpression in IPH PAECs decreased dihydroethidium (DHE) fluorescence, indicating decreased ROS formation. (C) NgBR knockdown in control PAECs decreased DAF fluorescence and (D) increased DHE fluorescence. L-NAME, N^ω-nitro-L-arginine methyl ester hydrochloride; SOD, polyethylene glycol-conjugated copper zinc superoxide dismutase. * $P < 0.05$ compared with empty plasmid; # $P < 0.05$ compared with L-NAME treated cells; † $P < 0.05$ compared with NS siRNA; ‡ $P < 0.05$ compared with cells not treated with SOD. Data are shown as mean (\pm SE).

$3.71 (\pm 0.48) \times 10^6$ RLU to $0.52 (\pm 0.05) \times 10^6$ RLU ($n = 5, P < 0.05$; Figure 4C), whereas DHE fluorescence increased from $2.84 (\pm 0.43) \times 10^6$ RLU to $7.01 (\pm 1.46) \times 10^6$ RLU ($n = 5, P < 0.05$; Figure 4D). The signals for DAF and DHE decreased significantly with N^G -nitro-L-arginine methyl ester hydrochloride and polyethylene glycol-SOD treatments, respectively, verifying the specificity of DAF staining for NO production and DHE staining for ROS formation. These results suggest that NgBR facilitates the regulation of NO and ROS formation in PAECs from developing lungs.

NgBR Modulates eNOS Coupling and the Levels of MnSOD and GTP-Cyclohydrolase-I Proteins

NO is an important upstream and downstream mediator of angiogenic factors involved in blood vessel formation. As shown in Figure 4A, NgBR overexpression rescued the attenuation of DAF fluorescence in IPH PAECs. This suggests

that NgBR facilitates coupled eNOS activity. Consistent with the results of NO levels, we observed increased eNOS serine¹¹⁷⁹ phosphorylation (0.64 ± 0.05 for NgBR overexpression versus 0.40 ± 0.05 for empty plasmid; $n = 3, P < 0.05$; Figure 5A), dimer formation (1.15 ± 0.07 for NgBR overexpression versus 0.71 ± 0.03 for empty plasmid; $n = 3, P < 0.05$; Figure 5B), and GTP-cyclohydrolase-I (GCH1) protein levels (0.16 ± 0.01 for NgBR overexpression versus 0.11 ± 0.01 for empty plasmid; $n = 3, P < 0.05$; Figure 5A) in IPH PAECs overexpressing NgBR. Total eNOS protein level did not change after NgBR overexpression. However, the signal for eNOS dimerization was low, and required the use of Femto mixed with Pico ECL (1:50) for detection of eNOS dimer in IPH PAECs. Increased eNOS phosphorylation at serine¹¹⁷⁹ and dimer formation are two well known indicators of eNOS activation (25, 26). In addition, GCH1 is the rate-limiting enzyme for the synthesis of tetrahydrobiopterin

(BH4), a required cofactor for coupled eNOS activity (25). Increased GCH1 protein levels suggest that NgBR overexpression facilitates eNOS recoupling in IPH PAECs.

Increased ROS formation by NADPH oxidase is known to contribute to the impaired angiogenesis in IPH PAECs (18, 26). We observed a decrease in DHE fluorescence in IPH PAECs overexpressing NgBR, suggesting decreased ROS formation (Figure 4B). However, we did not observe any change in the levels of NADPH oxidase subunits, either p47^{phox} or gp91^{phox} (Figure 5C). We observed a modest increase in MnSOD protein levels with the overexpression of NgBR (1.69 ± 0.10 for NgBR overexpression versus 1.27 ± 0.02 for empty plasmid; $n = 3, P < 0.05$; Figure 5C), which may lead to more efficient scavenging of ROS and increased NO bioavailability. Although the MnSOD protein levels only increased by one-third, MnSOD-specific activity in IPH PAECs increased significantly, by approximately

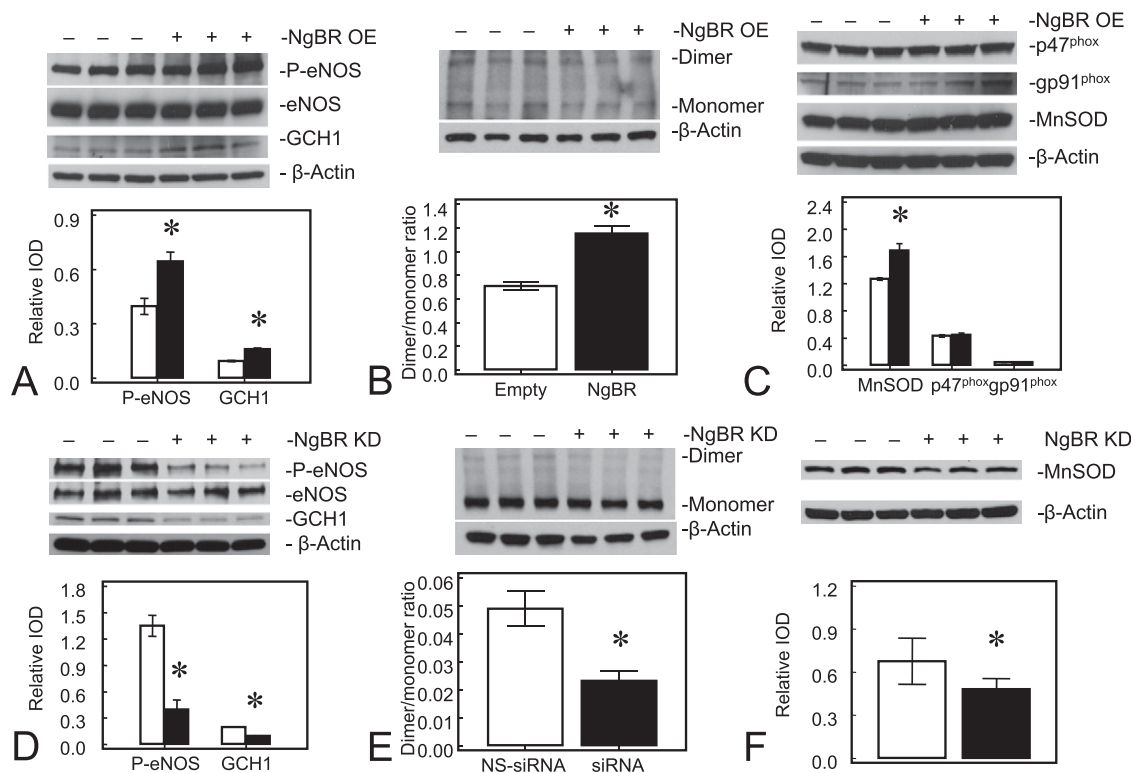


Figure 5. NgBR level modulates endothelial NO synthase (eNOS) phosphorylation and GTP-cyclohydrolase-1 (GCH1) and manganese superoxide dismutase (MnSOD) protein levels in PAECs. NgBR overexpression (OE) increased GCH1 protein level (A), eNOS phosphorylation, eNOS dimer formation (B), and MnSOD level (C) in IPH PAECs. NgBR knockdown (KD) decreased GCH1 level (D), eNOS phosphorylation (D) and dimer formation (E), and MnSOD level (F) in control PAECs. Open bar, control; closed bar, NgBR overexpression or knockdown. * $P < 0.05$ compared with control. Data are shown as mean (\pm SE).

56%, from $2.84 (\pm 0.12)$ to $4.43 (\pm 0.15)$ U/mg protein after NgBR overexpression ($n = 5, P < 0.05$). Our previous observation that impaired MnSOD transport into mitochondria contributes significantly to the decreased MnSOD activity in IPH PAECs may explain the discrepancy between MnSOD levels and MnSOD activity that we observed in this study (19).

To verify the role of NgBR in eNOS activation and ROS formation further, we performed NgBR knockdown in control PAECs. NgBR knockdown decreased eNOS phosphorylation (0.40 ± 0.11 for NgBR knockdown versus 1.35 ± 0.12 for NS siRNA; $n = 3, P < 0.05$) and GCH1 protein levels (0.10 ± 0.01 for NgBR knockdown versus 0.20 ± 0.01 for NS siRNA; $n = 3, P < 0.05$) in control PAECs (Figure 5D). There was no change in eNOS protein level, but dimer formation decreased after NgBR knockdown (0.02 ± 0.01 for NgBR knockdown versus 0.05 ± 0.01 for NS siRNA; $n = 3, P < 0.05$; Figure 5E). Similarly, NgBR knockdown decreased MnSOD protein levels in control PAECs (0.48 ± 0.02 for NgBR knockdown versus 0.67 ± 0.04 for NS siRNA; $n = 3, P < 0.05$; Figure 5E).

We investigated the mechanism(s) by which NgBR recouples eNOS in IPH PAECs further using VEGF stimulation. NgBR overexpression increased basal eNOS serine¹¹⁷⁹ phosphorylation and VEGF-stimulated eNOS phosphorylation by roughly 2.4-fold and roughly 1.9-fold, respectively, in IPH PAECs (Figure 6A). Parallel to the change in eNOS phosphorylation, NgBR overexpression also increased basal Akt phosphorylation and VEGF-stimulated Akt phosphorylation to roughly 2.5 fold and roughly 1.5-fold, respectively, in IPH PAECs (Figure 6A). NgBR knockdown in control PAECs resulted in reciprocal changes with decreased eNOS and Akt phosphorylation under basal and VEGF stimulation conditions (Figure 6B).

ROS Affect NgBR Levels in PAECs

We also investigated whether ROS affect NgBR levels in PAECs. We treated control PAECs with $40 \mu\text{M H}_2\text{O}_2$ every 8 hours, for 24 or 48 hours, to increase ROS formation, or treated IPH PAECs with $500 \mu\text{M N}$ -acetylcysteine (NAC), a thiol-containing antioxidant, every 24 hours for 48 hours to decrease ROS. H_2O_2 treatment of control PAECs decreased the NgBR protein levels

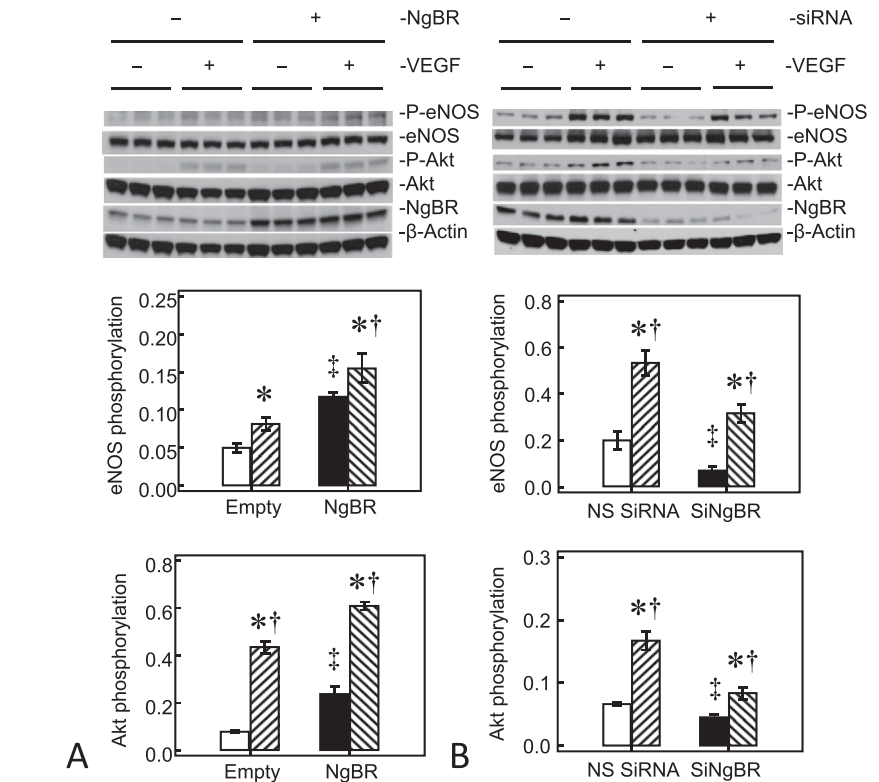


Figure 6. NgBR modulates eNOS coupling through Akt pathway. (A) NgBR overexpression in IPH PAECs increased the basal phosphorylation of eNOS and Akt, as well as vascular endothelial growth factor (VEGF)-stimulated phosphorylation of eNOS and Akt. (B) NgBR knockdown in control PAECs decreased the basal phosphorylation of eNOS and Akt, as well as VEGF-stimulated phosphorylation of eNOS and Akt. *Open bar*, empty plasmid or NS siRNA transfected unstimulated PAECs; *closed bar*, plasmid or siRNA transfected unstimulated IPH PAECs; *hatched bar*, VEGF-stimulated empty plasmid or NS siRNA transfected PAECs; *back-hatched bar*, VEGF-stimulated, plasmid, or siRNA transfected PAECs. * $P < 0.05$ compared with the corresponding unstimulated PAECs group for empty, NgBR plasmid or NS siRNA transfected cells; † $P < 0.05$ compared with empty plasmid or NS siRNA transfected, unstimulated PAECs; ‡ $P < 0.05$ compared with plasmid or siRNA transfected, unstimulated PAECs. Data are shown as mean (\pm SE).

at both 24 and 48 hours (0.41 ± 0.07 for H_2O_2 24 h versus 0.31 ± 0.03 for H_2O_2 48 h versus 0.81 ± 0.03 for control; $n = 3, P < 0.05$; Figure 7A). In contrast, NAC treatment of IPH PAECs increased the NgBR protein levels (0.14 ± 0.02 for NAC versus 0.06 ± 0.01 for untreated IPH PAECs; $n = 4, P < 0.05$; Figure 7B). These findings suggest that ROS levels in PAECs modulate the expression of NgBR in PAECs.

Discussion

Our study provides novel data on the role of NgBR in the evolution of IPH-related defects in blood vessel formation in the developing lungs. Our results show that NgBR levels are decreased, whereas Nogo-B is increased, in IPH lungs of fetal lambs,

a widely used model of PPHN, and that altered NgBR expression in PAECs impairs *in vitro* angiogenesis. We observed these alterations of NgBR in both cultured PAECs and in the intact lungs, suggesting that these changes are significant to the evolution of IPH. We also demonstrated that the altered NgBR expression in PAECs modulates NO levels and ROS formation by affecting eNOS coupling and MnSOD expression/activity, respectively. We previously reported that IPH PAECs have several phenotype changes, including eNOS uncoupling (17), decreased GCH1 expression and BH4 formation (25), decreased MnSOD expression and activity (19), and increased NADPH oxidase activity (18, 26). These phenotype changes in IPH PAECs lead to decreased NO and increased ROS formation, which together contribute to the impaired angiogenesis (18). The

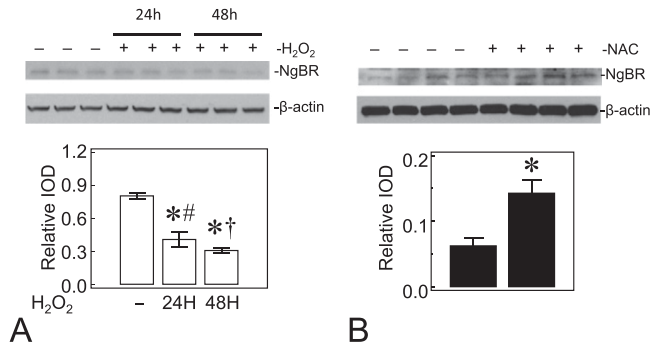


Figure 7. ROS affect the NgBR levels in PAECs. (A) H₂O₂ at 40 μM final concentration applied every 8 hours for 24 and 48 hours decreased the NgBR protein levels in control PAECs. (B) N-acetylcysteine (NAC) at 500 μM final concentration applied once every 24 hours for 2 days increased NgBR levels in IPH PAECs. Open bar, no treatment; closed bar, corresponding H₂O₂ or NAC treatment. **P* < 0.05 compared with no treatment; #*P* < 0.05 compared with 48 hours; †*P* < 0.05 compared with 24 hours. Data are shown as mean (± SE).

increased levels of MnSOD and GCH1 after NgBR overexpression in IPH PAECs may facilitate eNOS recoupling. As expected, these changes were associated with an observed improvement in angiogenesis. The molecular mechanism(s) by which NgBR increases MnSOD and GCH1 protein levels requires further investigation.

Our data also suggest that ROS formation affects the expression of NgBR in PAECs (Figure 7). Exposure to H₂O₂, which increases ROS levels in control PAECs (26, 28), has led to decreased NgBR protein levels, similar to our observation in IPH PAECs. In contrast, scavenging ROS by NAC increased the NgBR expression in IPH PAECs. Our findings suggest that ROS levels in IPH may contribute to decreases in NgBR expression in PAECs.

Although the ligand, Nogo-B, plays an important role in blood vessel formation

and maintenance, its depletion in mice is nonlethal (29). We hypothesized that NgBR may have more critical roles in modulating angiogenesis (13). As shown in our previous report (13), ablation of NgBR in zebrafish resulted in more severe defects of intersomitic blood vessel formation compared with the defects caused by Nogo-B deficiency (29). In addition, NgBR knockdown in human umbilical vein endothelial cells not only abolished Nogo-B-stimulated cell migration, but also reduced VEGF-stimulated cell migration (13). These data suggest that NgBR is also essential for other angiogenic factors besides Nogo-B. Here, our results demonstrated that changes in NgBR expression altered the *in vitro* angiogenesis of PAECs. Mechanistically, the increased MnSOD expression and activity in IPH PAECs overexpressing NgBR may lead to

decreased ROS levels and increased NO bioavailability. Increased GCH1 levels observed in IPH PAECs with NgBR overexpression may help recouple eNOS by increased BH₄ formation (25). This possibility is further supported by increased eNOS ser¹¹⁷⁹ phosphorylation and dimer formation, NO levels, and decreased ROS formation after NgBR overexpression in the IPH PAECs. The observed changes in Akt phosphorylation after changes in NgBR expression strongly suggest that NgBR also modulates Akt/eNOS signaling pathway. The detailed molecular mechanism by which NgBR regulates expression of GCH1 and MnSOD, as well as phosphorylation of Akt and eNOS, requires further investigation.

In conclusion, our data demonstrate that NgBR modulates angiogenesis in the developing lungs through increased Akt/eNOS activity and MnSOD expression/activity in PAECs. To the best of our knowledge, this is the first report of a relationship between NgBR expression and eNOS activation. Our study provides new insights into the mechanistic role of NgBR in the impaired angiogenesis in IPH. Further understanding of the molecular mechanisms by which IPH decreases NgBR expression may facilitate development of new therapeutic approaches to restore lung growth in IPH. ■

Author disclosures are available with the text of this article at www.atsjournals.org.

Acknowledgments: The authors thank Jacek Zielonka, Ph.D., for helping in quantification of reactive oxygen species formation.

References

- Oertle T, Schwab ME. Nogo and its parTners. *Trends Cell Biol* 2003;13:187–194.
- Yang YS, Strittmatter SM. The reticulons: a family of proteins with diverse functions. *Genome Biol* 2007;8:234.
- Ng CE, Tang BL. Nogos and the Nogo-66 receptor: factors inhibiting CNS neuron regeneration. *J Neurosci Res* 2002;67:559–565.
- Teng FY, Tang BL. Cell autonomous function of Nogo and reticulons: the emerging story at the endoplasmic reticulum. *J Cell Physiol* 2008;216:303–308.
- Dodd DA, Niederoest B, Bloechlinger S, Dupuis L, Loeffler J-P, Schwab ME. Nogo-A, -B, and -C are found on the cell surface and interact together in many different cell types. *J Biol Chem* 2005;280:12494–12502.
- Schwab ME. Functions of Nogo proteins and their receptors in the nervous system. *Nat Rev Neurosci* 2010;11:799–811.
- Pan J-W, Zheng X, Yang P-Y, Qin Y-W, Rui Y-C, Ma L-P, Zhou F, Kang H. Different expressions of Nogo-B1 and Nogo-B2 in mouse heart microvascular endothelial cell dysfunction induced by lysophosphatidylcholine. *Microvasc Res* 2006;72:42–47.
- Kim JE, Bonilla IE, Qiu D, Strittmatter SM. Nogo-C is sufficient to delay nerve regeneration. *Mol Cell Neurosci* 2003;23:451–459.
- Josephson A, Trifunovski A, Widmer HR, Widenfalk J, Olson L, Spenger C. Nogo-receptor gene activity: cellular localization and developmental regulation of mRNA in mice and humans. *J Comp Neurol* 2002;453:292–304.
- Acevedo L, Yu J, Erdjument-Bromage H, Miao RQ, Kim JE, Fulton D, Tempst P, Strittmatter SM, Sessa WC. A new role for Nogo as a regulator of vascular remodeling. *Nat Med* 2004;10:382–388.
- Yu J, Fernández-Hernando C, Suarez Y, Schleicher M, Hao Z, Wright PL, DiLorenzo A, Kyriakides TR, Sessa WC. Reticulon 4B (Nogo-B) is necessary for macrophage infiltration and tissue repair. *Proc Natl Acad Sci USA* 2009;106:17511–17516.
- Miao RQ, Gao Y, Harrison KD, Prendergast J, Acevedo LM, Yu J, Hu F, Strittmatter SM, Sessa WC. Identification of a receptor necessary for Nogo-B stimulated chemotaxis and morphogenesis of endothelial cells. *Proc Natl Acad Sci USA* 2006;103:10997–11002.
- Zhao B, Chun C, Liu Z, Horswill MA, Pramanik K, Wilkinson GA, Ramchandran R, Miao RQ. Nogo-B receptor is essential for angiogenesis in zebrafish via Akt pathway. *Blood* 2010;116:5423–5433.

14. Geggel RL, Reid LM. The structural basis of PPHN. *Clin Perinatol* 1984; 11:525–549.
15. Morin FC III. Ligating the ductus arteriosus before birth causes persistent pulmonary hypertension in the newborn lamb. *Pediatr Res* 1989;25:245–250.
16. Konduri GG, Ou J, Shi Y, Pritchard KA Jr. Decreased association of HSP90 impairs endothelial nitric oxide synthase in fetal lambs with persistent pulmonary hypertension. *Am J Physiol Heart Circ Physiol* 2003;285:H204–H211.
17. Konduri GG, Bakhutashvili I, Eis A, Pritchard K Jr. Oxidant stress from uncoupled nitric oxide synthase impairs vasodilation in fetal lambs with persistent pulmonary hypertension. *Am J Physiol Heart Circ Physiol* 2007;292:H1812–H1820.
18. Teng RJ, Eis A, Bakhutashvili I, Arul N, Konduri GG. Increased superoxide production contributes to the impaired angiogenesis of fetal pulmonary arteries with *in utero* pulmonary hypertension. *Am J Physiol Lung Cell Mol Physiol* 2009;297:L184–L195.
19. Afolayan AJ, Eis A, Teng RJ, Bakhutashvili I, Kaul S, Davis JM, Konduri GG. Decrease in manganese superoxide dismutase expression and activity contribute to oxidative stress in persistent pulmonary hypertension of the newborn. *Am J Physiol Lung Cell Mol Physiol* 2012;303:L870–L879.
20. Mi Y-J, Hou B, Liao Q-M, Ma Y, Luo Q, Dai Y-K, Ju G, Jin W-L. Amino-Nogo-A antagonizes reactive oxygen species generation and protects immature primary cortical neurons from oxidative toxicity. *Cell Death Differ* 2012;19:1175–1186.
21. Sutendra G, Dromparis P, Wright P, Bonnet S, Haromy A, Hao Z, McMurtry MS, Michalak M, Vance JE, Sessa WC, *et al.* The role of Nogo and the mitochondria–endoplasmic reticulum unit in pulmonary hypertension. *Sci Transl Med* 2011;3:88ra55.
22. Hoyer LW, De los Santos RP, Hoyer JR. Antihemophilic factor antigen: localization in endothelial cells by immunofluorescent microscopy. *J Clin Invest* 1973;52:2737–2744.
23. Voyta JC, Via DP, Butterfield CE, Zetter BR. Identification and isolation of endothelial cells based on their increased uptake of acetylated-low density lipoprotein. *J Cell Biol* 1984;99: 2034–2040.
24. Feliers D, Chen X, Akis N, Choudhury GG, Madaio M, Kasinath BS. VEGF regulation of endothelial nitric oxide synthase in glomerular endothelial cells. *Kidney Int* 2005;68:1648–1659.
25. Teng RJ, Du J, Xu H, Bakhutashvili I, Eis A, Shi Y, Pritchard KA Jr, Konduri GG. Sepiapterin improves angiogenesis of pulmonary artery endothelial cells with *in utero* pulmonary hypertension by recoupling endothelial nitric oxide synthase. *Am J Physiol Lung Cell Mol Physiol* 2011;301:L334–L345.
26. Teng RJ, Du J, Welak S, Guan T, Eis A, Shi Y, Konduri GG. Cross talk between NADPH oxidase and autophagy in pulmonary artery endothelial cells with intrauterine persistent pulmonary hypertension. *Am J Physiol Lung Cell Mol Physiol* 2012;302: L651–L663.
27. Pritchard KA Jr, Ackerman AW, Gross ER, Stepp DW, Shi Y, Fontana JT, Baker JE, Sessa WC. Heat shock protein 90 mediates the balance of nitric oxide and superoxide anion from endothelial nitric-oxide synthase. *J Biol Chem* 2001;276:17621–17624.
28. Zinkevich NS, Gutterman DD. ROS-induced ROS release in vascular biology: redox–redox signaling. *Am J Physiol Heart Circ Physiol* 2011;301:H647–H653.
29. Kim JE, Li S, GrandPré T, Qiu D, Strittmatter SM. Axon regeneration in young adult mice lacking Nogo-A/B. *Neuron* 2003;38: 187–199.